

Flexural Retrofitting Design for Strength and Debonding Prevention

G.X. Guan¹, C.J. Burgoyne²

¹Assistant Engineer, Gammon Construction Ltd. Hong Kong, Garfieldkwan@gmail.com

²Reader of Concrete Structure, University of Cambridge, UK, cjb@eng.cam.ac.uk

Keywords: CFRP; Beam; Flexural strengthening; Debonding; Structural Design

SUMMARY

In flexural retrofitting of RC beams using CFRP plate, there is a lack of methods to determine where the strengthening plate can safely be curtailed. As a result, retrofitted beams commonly fail by debonding of the FRP plate before the target flexural capacity. Global Energy Balance Approach (GEBA) using fracture mechanics has been proposed to determine the debonding load of an FRP-RC beam. The GEBA results for various FRP-RC beams can be summarised using debonding contours on plots of moment capacity against the safe plate curtailed locations. This paper shows how GEBA can be incorporated into the design process to prevent premature debonding of the CFRP plate. The method makes use of the debonding contours and derives from these simplified design charts that could be made available to designers. The retrofitting design consideration and the theoretical background of this unified design method are first explained, followed by the derivation of the conceptual design charts. Numerically correct design charts are then constructed for a wide range of design cases, and a worked example is given at the end.

1. INTRODUCTION

FRP plates can be used to enhance the capacity of under-reinforced RC beams to make the beams stronger but has the effect of reducing the ductility. Retrofitted beams are known to suffer from premature debonding at loads below their design strength. Fig. 1 shows typical moment curvature relationships for three beams. Curve (A) applies to an unstrengthened under-reinforced beam; it has a relatively long plateau at virtually constant load as the steel yields before the concrete crushes. Curve (B) shows the effect of adding a moderate amount of strengthening; the beam yields at a higher load because of the presence of the CFRP, and continues to resist more load after the steel yields because the CFRP remains elastic. However, final crushing of the concrete occurs at a lower deflection because the neutral axis is deeper. The limiting case is shown in curve (C) for a balanced section, where the concrete crushes at the same time as the steel yields.

The original service load is shown as P_{u-s} while the original ultimate load capacity is P_{u-u} . There are several limits on the amount of flexural strengthening that is possible.

1. Most beams are under-reinforced to prevent brittle failure. The beam should not be strengthened to such an extent that it now becomes over-reinforced, so one limit on the amount of FRP gives the corresponding balanced section design (Curve C).
2. It is undesirable for the beam to undergo plastic deformation under normal service loads to avoid incremental plasticity, so the retrofitted service load limit (P_{s-y}) is calculated from the moment that causes first yield of the original steel reinforcement, typically at mid-span where the moment is highest. Hence the retrofitted service load (P_{s-s}) should always be less than the strengthened yielding capacity. The real increase in load capacity is then given by $P_{s-s} - P_{u-s}$. The increase of

- strengthened ultimate capacity ($P_{s-u} - P_{u-u}$) is greater than the increase in yielding capacity ($P_{s-y} - P_{u-y}$) because of the gain in stress in the CFRP after the steel has yielded.
- The theoretical ultimate strength P_{s-u} cannot be used at the working load but it may be needed to provide adequate reserve of strength if the beam is overloaded. The FRP plate rupture strain is typically much greater than the steel yield strain, so the beam would fail by concrete crushing. This is the beam's ultimate state.
 - The increase in flexural capacity should not alter the ultimate failure state from flexure to shear.

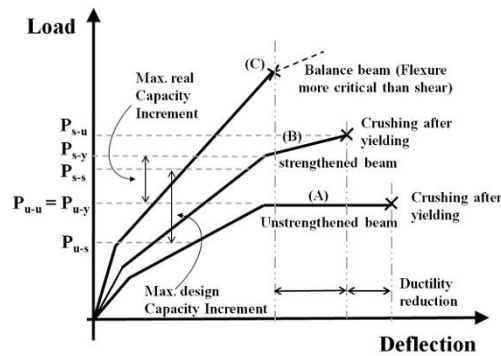


Figure 1 Considerations in FRP retrofitting design

Tests have shown that plate end (PE) debonding, which initiates from a horizontal crack near the plate end in the concrete cover, is a common mechanism of failure for retrofitted beams. It is essential that PE debonding does not occur, not only when the steel is elastic but also be adequate when the steel is yielding. PE debonding can normally be prevented by extending the FRP plate towards the support, but it is important to know how long the plate should be. The designer needs to choose the curtailment location L_{cur} in such a way that premature PE debonding is prevented.

In order to prevent premature PE debonding different innovative techniques have been proposed, for example: (i) to extend the FRP plate towards the supports [1,2], (ii) to wrap FRP sheets around the beam or the web to reduce the beam cracks [3,4], (iii) to anchor the FRP plate end into the beam by additional FRP straps [5], and (iv) to incorporate various anchorage systems such as bolting [6,7]. Although they are helpful in some extent, these inventions are far from mature and some are not practical: at the same time they aim to prevent debonding rather than to understand it.

Unlike intermediate-crack-induced (IC) debonding, which is commonly prevented by limiting the section strains, PE debonding normally initiates well away from the load, at a place where the flexural strains are small. Strain criteria are thus not relevant. A study based on fracture analysis of concrete, which relates the change in the strain energy in the beam and the potential energy of the load to the energy that is released in the concrete when the fracture propagates, has been used to predict when debonding would occur. This is known as the Global Energy Balance Approach (GEBA), and have been used by different researchers [8-11]. The key comparison is between the Energy Release Rate G_R with the Fracture Energy of Concrete G_f . The particular value of G_f is normally well within the range from 0.05 to 0.3 N/mm [12,13].

A parametric study of GEBA has been presented by the authors in [14], where debonding contour (DBC) plots have been used as the PE debonding criterion: G_R varies as a function of the loading state at which debonding occurs, and as a function of where the fracture takes place. G_R is determined from M- κ models, so the DBC can be plotted on a graph of normalised moment capacity ($M/f_c'bd^2$) and curtailment location (L_{cur}/L_{shear}), which allows the strength design and the debonding design to be combined, as shown in Fig. 2.

The DBC is where the G_R surface intercepts the horizontal plane that is defined by G_f . The DBC varies for beams with different depths, reinforcing steel, FRP material etc. A detailed discussion of the DBC is found in [14], where it was shown that a normalized debonding criterion using a ratio of

beam depth and fracture energy (h/G_f) could be used for design. A step-by-step illustration of the design approach is given below.

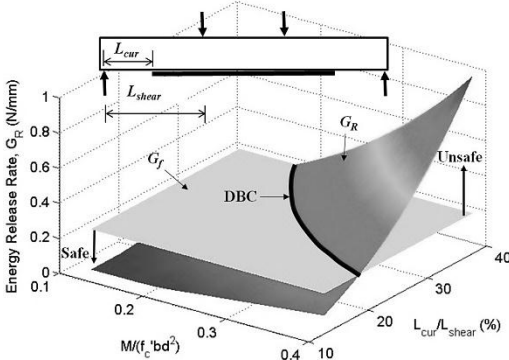


Figure 2 Determination of DBC

2. UNIFIED RETROFITTING DESIGN APPROACH

It is straightforward to design the amount of FRP required using simple beam theory by assuming that the FRP plate acts as a second layer of fully-bonded reinforcement. It has been recognised that debonding prevention is much more complicated as explained in [8,15]. Here, it is achieved using the DBC obtained from GEBA.

2.1. Design method and schematic charts

In a typical contour plot (Fig.3), the state of an FRP-RC beam with a given FRP plate curtailment length (L_{cur}/L_{shear}) under a particular design load ($M/f'_c b d^2$) at midspan is represented by a data point called beam state point (BSP). It is necessary to establish the safe region for the BSP. The strength limit is obtained from flexural design, by checking when first yielding of the steel occurs at midspan, which gives a limiting value for the applied moment: it is represented by the vertical yielding line (YL). The debonding criterion limits L_{cur}/L_{shear} by means of the DBC. The regions where flexural or debonding failure might occur are shown. The BSP must lie within the shaded region to keep the beam safe.

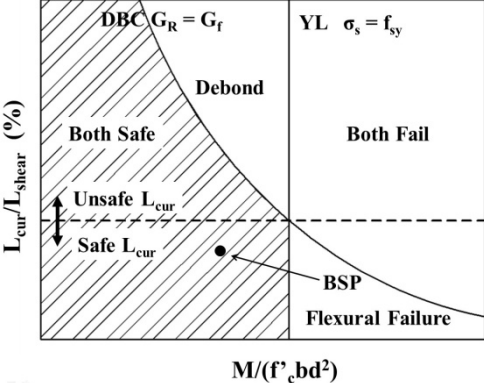


Figure 3 The four regions for BSP defined from CBD and YL

For reasons of economy, it is desirable that the strengthening should bring the section as close as possible to the YL line. Therefore, the value of L_{cur}/L_{shear} should be lower than the value given by the dashed line that passes through the intersection of the DBC and YL. This defines a limiting maximum curtailment length. If a beam is designed such that BSP lies above this dashed line, premature debonding occurs before the beam’s flexural capacity is reached. Because the unstrengthened beam was under-reinforced, debonding prevention is mainly a function of the tension steel ratio (ρ_s) and the FRP ratio (ρ_f). To strengthen a particular RC beam, ρ_s is fixed but the designer can change ρ_f , whereas when considering different RC beams ρ_s also varies. The effect of these two changes are shown

separately in Figs 4 (a) and (b); adding either type of reinforcement always moves YL to the right (YL1 to YL2), but it has different effects on the DBC. Increasing ρ_f means that debonding occurs more easily so the debonding line moves. In contrast, with a larger ρ_s , debonding is less likely. The maximum curtailment ($L_{cur-max}$) changes correspondingly.

In order to make the above design charts cover a wide range of design cases, say for ρ_s from 0.4 to 2.0% and ρ_f from 0.1 to 1.5%, a very large number of DBCs and YLs would be needed and the charts would be very complicated. However, it is noted that the critical point is the intersection point of the DBC and YL. Any designed BSP below and to the left of this point is safe, which leads to the simpler design charts described below.

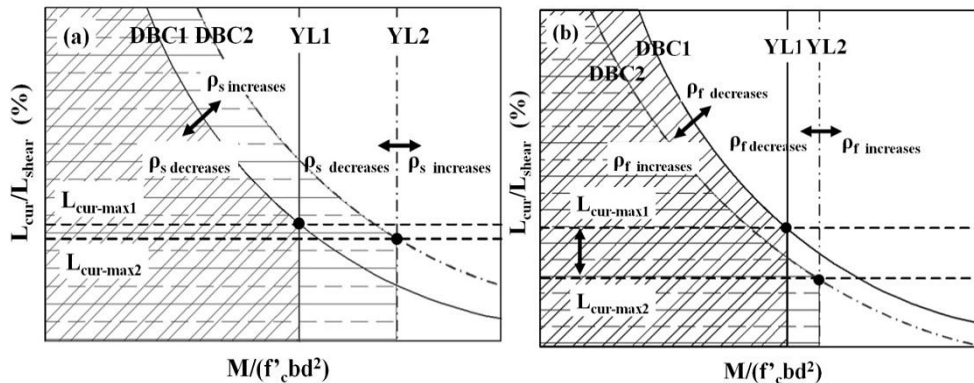


Figure 4 (a) Change of the 'Both safe' region with increasing ρ_s (b) Change of the 'Both safe' region with increasing ρ_f

2.2. Simplified design method and schematic charts

Simplified design for pre-yielding stage

The intercepts of the DBCs and the YLs are used to construct simplified design charts as illustrated in Fig. 5(a): Firstly, keep ρ_f constant and vary ρ_s continuously. The locus of intercepts of the DBC's and the YL's form a curve. This track of intercepts is named the steel-ratio track of intercepts (STI). A family of STI can be constructed by repeating the above step for different ρ_f values. With a set of STIs, the variation of ρ_s is represented by the movement of a point along one STI, and the change of ρ_f is the change between different STIs. It is noted that if the moment is reduced, the STI line gets higher, which implies that L_{cur} could be higher, but the DBC also gets higher, but more steeply (Fig. 5(b)). So if the user chooses to use the STI line for design the FRP will not debond before yielding. However, the STI cuts into the unsafe region in post-yielding stage so that it should not be used for post-yielding design.

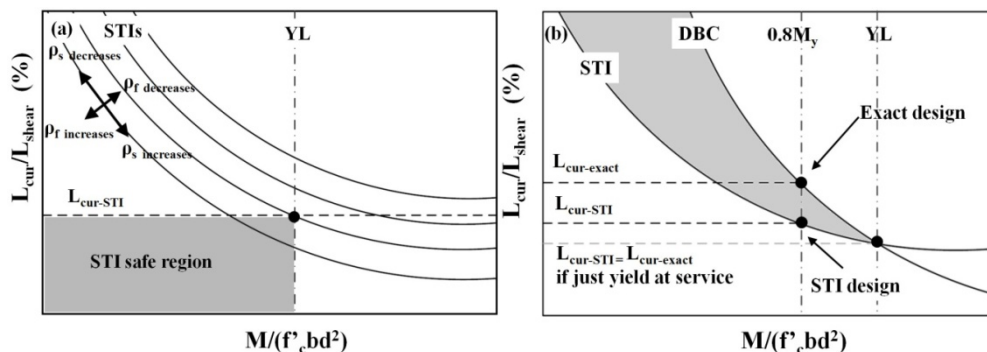


Figure 5 (a) Conceptual design chart with ST; (b) Comparison between STI design and the exact design

Simplified design for post-yielding stage

Although the service load must occur while the steel is still elastic, it has already been mentioned that the beams may have to carry loads above yield in order to provide sufficient reserve of strength. It is

essential that the FRP does not debond before the ultimate strength of the beam is reached. This can be accomplished by means of a different set of curves, which are constructed in the same way as the STI curves, by varying ρ_f only, giving the FRP-ratio track of intercepts (FTI) (Fig. 6(a)). The increase of ρ_s makes debonding less likely while an increase of ρ_f makes it more likely. Graphically, FTI and STI curves have a similar trend but different inclinations and for a particular combination of (ρ_s, ρ_f) they cross each other at the yielding state. In the pre-yielding stage, the STI line lies below the DBC, so for design purposes it gives conservative results. Beyond yield, the FTI lines are below the DBC, and thus are conservative (Fig. 6(b)). If the reserve of strength that is required beyond yield is high, it is possible that a negative curtailment is predicted as shown in Fig. 6(b) (no positive intercept for the FTI at $1.5M_y$). This indicates that an anchorage is required in addition to the bond.

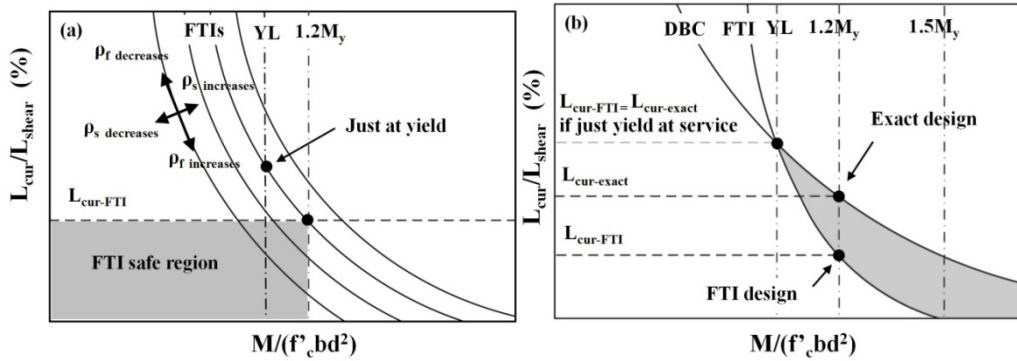


Figure 6 (a) Conceptual design chart with FTI; (b) Comparison between FTI design and the exact design

2.3. Unified design procedures

The area of steel is known, so ρ_s is fixed

1. Simple beam theory is applied to determine the amount of FRP needed to satisfy the requirements for both the service load (when the steel must not yield), and the ultimate load (when it probably will). The higher value of A_f and hence ρ_f are chosen.
2. The designer uses the STI curves to determine L_{cur} at the service load, and the FTI curves to determine L_{cur} at the ultimate load.

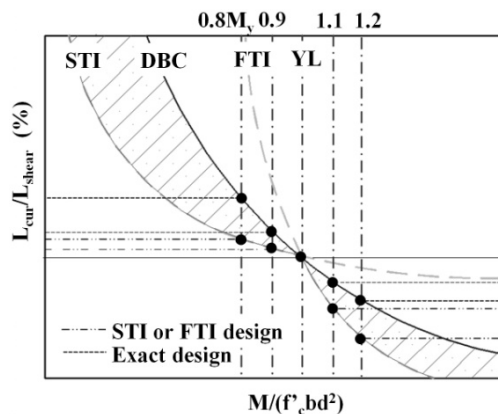


Figure 7 Comparison of the exact design, and design based on STI and FTI

Fig. 7 illustrates these principles by combining the STI and FTI curves, together with the DBC. If the designer wished to do an exact design, the maximum allowable curtailment is given by the intersection of the applied moment and the DBC, shown by the dotted line in Fig. 7. To obtain a DBC requires complicated computation, and each DBC corresponds to only one design scenario so there are too many DBCs to be provided for design charts. Meanwhile, STI and FTI are compacted charts that can be provided as design charts to cover a wide range of design scenarios but are more conservative. The chain-dotted lines in Fig. 7 show how the curtailment locations would be chosen using the simplified method. The values of L_{cur}/L_{shear} obtained from the simplified method are always below the exact

values, and are thus safer. The hatched areas are the marginally safe areas that may be used to design the FRP-RC beam to a more economical or more extreme capacity state. A detailed worked example is provided at the end to show how an FRP retrofitting design is made using this proposed method.

3. DETAILED DESIGN CHART CONSTRUCTION

The charts given below are constructed for beams with cylindrical concrete strength $f'_c = 37$ MPa, with steel yield strength $f_y = 530$ MPa and Young's modulus $E_s = 200$ GPa, and with FRP elastic modulus $E_f = 165$ GPa. The STI and FTI are the locus of intersections of YLs and DBCs. Here the YLs are constructed assuming the tension steel yields at the strain f_y/E_s , the FRP plate behaves elastically, and the concrete in compression follows an unfactored parabolic stress-strain relationship in [16]. When considering DBC, the most important parameter is the ratio h/G_f (MPa⁻¹). It was shown in [14] that DBCs for beams with the same h/G_f value are virtually identical. Thus the DBCs and the resulting STI and FTI charts below apply to all the beams having the same h/G_f .

3.1. Construction of detailed STI design charts

The STI curves can give a conservative design curtailment in the pre-yielding stage, so that they are used to consider debonding prevention for the service state. Fig. 8(a) shows a typical STI design chart that relates to a 400 mm deep beam, with G_f taken as 0.15 N/mm, so $h/G_f = 2.67 \times 10^3$ MPa⁻¹. It has been produced by keeping ρ_f constant (at 0.5%) and varying ρ_s continuously. The family of thin curved lines are the DBCs for different values of ρ_s , while the different vertical dashed lines are the corresponding YL lines. The darker curved line is the STI which goes through the intersections of the corresponding pairs of DBCs and YLs. The darker solid (vertical) line relates to $\rho_s = 1.0\%$. One STI curve covers the retrofitted design of a beam with a certain depth and ρ_f value, but various ρ_s values.

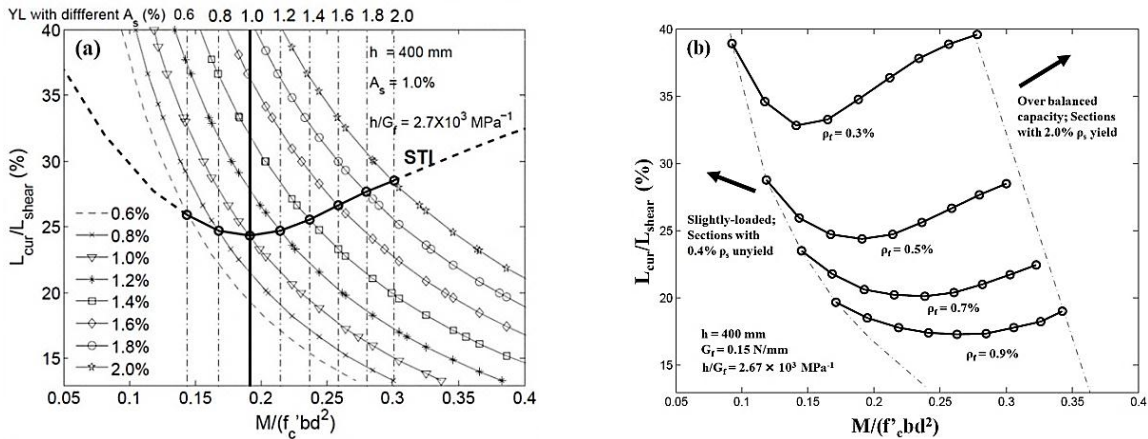


Figure 8 (a) Construction of STI for beam having $h = 400$ mm and $G_f = 0.15$ N/mm; (b) Numerically correct STI for 400 mm deep beam ($h/G_f = 2.7 \times 10^3$ MPa⁻¹)

Design charts can be produced by repeating the process used to find Fig. 8(a) for different ρ_f values, to give a family of STIs for beams with a fixed value of h/G_f . Fig. 8(b) shows such a plot for $h/G_f = 2.67 \times 10^3$ MPa⁻¹ and $h = 400$ mm. The darker curves are the exact STIs, covering the range of ρ_s from 0.4% to 2.0%. It is evident from the figures that if a lot of FRP is present, (for example $\rho_f = 0.9\%$), PE debonding is likely and the plate must be extended close to the support (L_{cur}/L_{shear} is small). If less FRP is needed, PE debonding is less likely and the plate can be curtailed further away from the support (L_{cur}/L_{shear} is larger).

3.2 Construction of detailed FTI design charts

The FTI curves can give a conservative design curtailment in the post-yielding stage and thus they are adopted to consider debonding that ensures the ultimate capacity. They are constructed in a similar manner to the STI charts, but this time keeping ρ_s constant and varying ρ_f continuously. Fig. 9(a) relates to a beam of 400 mm deep, with G_f taken as 0.15 N/mm. By repeating the process for different

ρ_s , a family of FTI is given to cover all the design cases for 400 mm deep beams with h/G_f value as $2.67 \times 10^3 \text{ MPa}^{-1}$, as in Fig. 9(b).

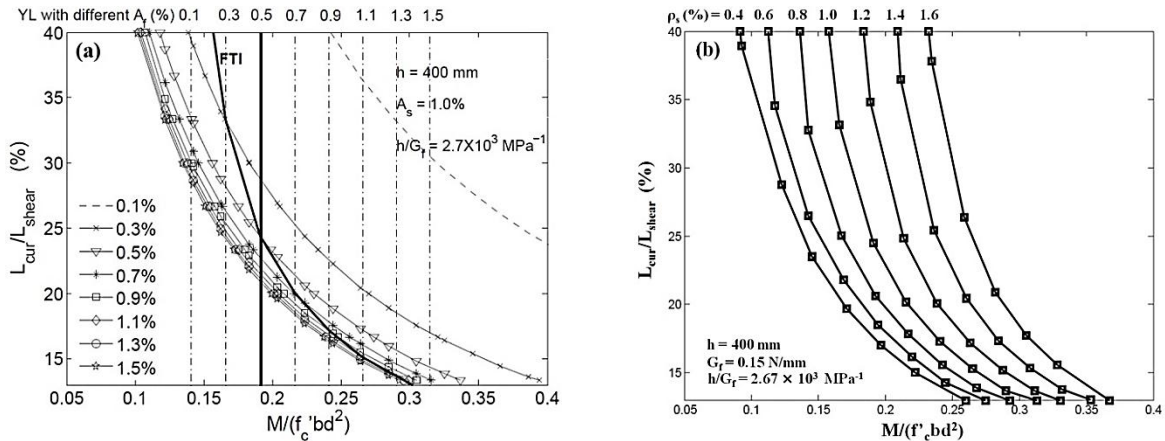


Figure 9 (a) Construction of FTI for beam having $h = 400 \text{ mm}$ and $G_f = 0.15 \text{ N/mm}$; (b) Numerically correct FTI for 400 mm deep beam ($h/G_f = 2.67 \times 10^3 \text{ MPa}^{-1}$)

3.3. Significance of the simplified design

A pair of STI and FTI Band charts is required for one design to consider both service state and ultimate state. Since h/G_f typically has a value in the range $0.5 - 20 \times 10^3 \text{ MPa}^{-1}$ for beams ranging from 200 to 1000 mm deep, and having a G_f ranging from 0.05 to 0.30 N/mm, in total, about ten pairs of STI and FTI Band charts are able to cover most design scenarios. Thus, the simplified design with STI and FTI Band charts provides a convenient way for practical engineering.

The effects of varying FRP elastic modulus is equivalent to varying the amount of FRP with a certain elastic modulus, since FRP is always elastic. On top of these STI and FTI Band charts, the change of material properties such as the concrete strength (f_c') and the steel yielding strength (f_y) will lead to variations.

4. WORKED EXAMPLE

A typical problem faced in a design office is to retrofit an existing beam. The design details of a one-span simply-supported beam that requires retrofitting is shown in Fig 10.

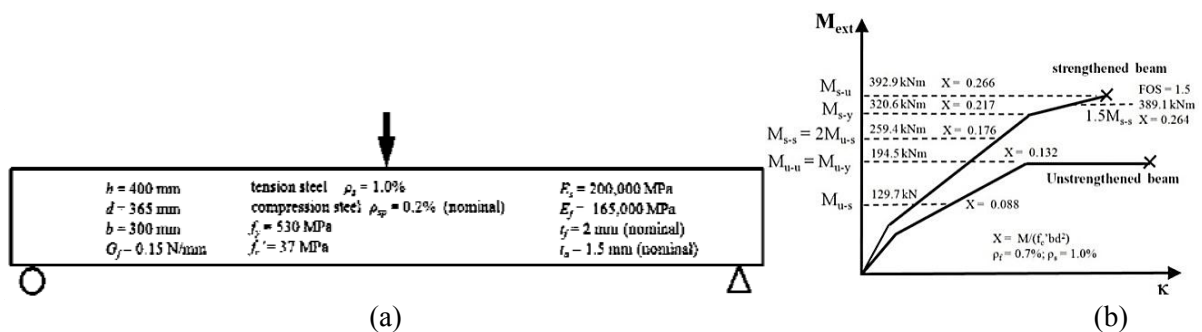


Figure 10 (a) Parameters for beam design (b) Summary of the flexural retrofitting design results

The calculations in the Appendix show that its original ultimate moment capacity (M_{u-y}) is assessed to be 194.5 kNm, which with a factor of safety of 1.5 gives an unstrengthened working load capacity (M_{u-s}) of 129.7 kNm. Suppose it is now required to take twice its original service load, which implies that the strengthened service load (M_{s-s}) should be 259.4 kNm. If it is to retain a factor of safety of 1.5 at ultimate this implies that M_{s-u} should exceed 389.1 kNm. The results of the retrofitting design to raise the flexural capacity are summarised in Fig. 10 (b): the upper and lower curves represent the behaviours of the strengthened and unstrengthened beams respectively. By adding 0.7% FRP ($\rho_f =$

0.7%) to the original beam, the beam is able to take over twice the original service load before the tension steel yields ($M_{s-y} > M_{s-s}$), and has a FOS over 1.5 at the ultimate state ($M_{s-u} > 1.5M_{s-s}$).

It is now necessary to use the principles outlined in this paper to determine where the FRP can be curtailed. When debonding is considered, the unified design method is applied. The design charts provided will be the STI and FTI charts (Figs 8 and 9). The critical number that determines which sets of design charts to use is h/G_f , which is $400/0.15 = 2.67 \text{ MPa}^{-1}$ in this case. Figure 11(a) is a reproduction of Fig. 8(b), but with the relevant lines highlighted. For the service state, a vertical line is first drawn at $M/(f_c'bd^2) = 0.176$ which represents the moment capacity required at service after retrofitting. Then the maximum curtailment in the problem is found to be 21.5% L_{shear} .

When considering the ultimate state, the FTI band charts are used for debonding prevention; Fig. 11(b) is a reproduction of Fig. 9(b), again with the relevant lines highlighted. Following the same procedures, the maximum curtailment for the beam is estimated as $L_{cur}/L_{shear} = 16.0\%$. Consequently, the ultimate state governs the debonding prevention, and the FRP plate should be curtailed less than 16.0% of the shear span away from the supports.

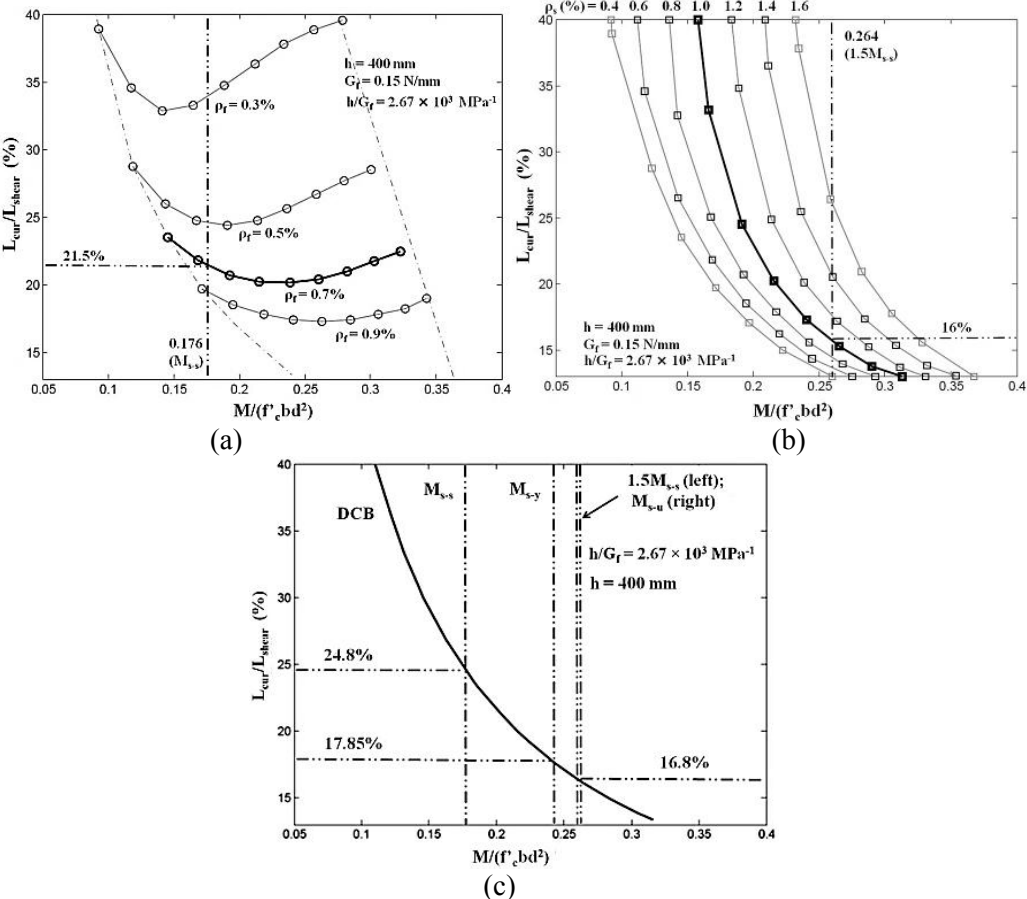


Figure 11 Determination of the curtailment from (a) STI, (b) FTI and (c) DCB design charts

The exact maximum curtailment obtained from DBC charts (exact design) is also provided here (Fig. 11(c)). The maximum values of L_{cur}/L_{shear} given by the exact design at service and ultimate states are 24.8% (intercepting M_{s-s}) and 16.8% (intercepting $1.5M_{s-s}$) respectively, which are greater than those predicted by simplified design above. Furthermore, if the FRP plate is curtailed to 17.8% of the shear span, it debonds when the tension steel yields. If the FRP plate is curtailed to 16.8%, debonding and crushing of compressive concrete occur almost simultaneously with the ultimate failure mechanism, since in this case $M_{u-s} (= 0.266)$ is close to $M_{s-s} (= 0.264)$. These values all exceed the value of 16.0% given by the simplified design charts. It should be noted that the DBC curves would not generally be

available to designers, whereas it is suggested that simplified STI and FTI band charts could be provided.

If the FRP ratio initially guessed cannot provide enough flexural capacity at service or ultimate state, it should be increased. However, an increase in FRP ratio reduces the critical curtailment length, which means the plate has to be placed closer to the supports. If the space for the extension of the FRP plate is the primary constraint, debonding prevention consideration will govern the retrofitting design, and the FRP ratio should be kept as small as possible. Otherwise, additional mechanical anchorage is needed to prevent premature debonding.

CONCLUSIONS

This paper proposes a unified design method for FRP retrofitting design considering flexural capacity and plate end debonding prevention simultaneously. In this design method, the flexural consideration is based on conventional beam theory to select the proper amount of FRP, represented by the normalized section capacity ($M/f_c'bd^2$) in terms of yielding line (YL) in charts. Assessment of PE debonding is based on concrete fracture analysis, applying the debonding contour (DBC). A retrofitting designer then has to select the proper amount of FRP material and the curtailment to make a beam fall into the safe region given by the combination of YL and DBC. A more concise simplified design chart is proposed to cover a large range of design cases for beams with different depths, different reinforcement ratios, various amount of FRP material, and in both service and ultimate states. This new approach provides a way of incorporating a fracture mechanics approach to debonding in a conventional beam design.

APPENDIX Flexural capacity design for the beam in the worked example

STEP 1 Assessment of original capacity

The original design flexural capacity corresponds to the first yield of the section. The concrete compression is calculated using an equivalent rectangular stress distribution according to ACI318-08. From force equilibrium:

$$0.85 \times 0.77 \times f_c'bx + \rho_{sp}bdE_s\varepsilon_{sp} = \rho_s bdf_y \quad (A1)$$

$$\text{where } \varepsilon_s = f_y / E_s = 0.00265 \text{ and } \varepsilon_{sp} = \frac{x - d_p}{d - x} \varepsilon_s$$

Substituting values and solving gives:

$$x = 77.5 \text{ mm}; F_{cc} = 563.2 \text{ kN}; F_{sc} = 17.2 \text{ kN}; F_{st} = 580.4 \text{ kN}.$$

The moment capacity of this unstrengthened section (at yield) is thus:

$$M_{u-u} = M_{u-y} = F_{st}(d - 0.5 \times 0.77x) = 580.4 \times (365 - 0.5 \times 0.77 \times 77.5) = 194.5 \text{ kNm} \quad (A2)$$

STEP 2 Design of amount of strengthening

The beam is now to be strengthened so that $M_{s-s} = 259.4 \text{ kNm}$, and $M_{s-u} > 1.5 M_{s-s}$ so is 389.1 kNm . After some trial and error it is found that FRP plate having a cross-sectional area equal to 0.7% of the beam section ($\rho_f = 0.7\%$) is will provide the necessary strengthening. This amount of FRP is OK, by checking the new service and ultimate conditions.

At service load, the tension steel in the strengthened beam (FRP-RC) just yields; this should occur at a moment greater than M_{s-s} . Using the method above, the section gives:

$$x = 127.1 \text{ mm}; F_{cc} = 923.4 \text{ kN}; F_{sc} = 44.9 \text{ kN}; F_{st} = 580.4 \text{ kN}; F_p = 388.0 \text{ kN}.$$

$$M_{s-y} = 320.6 \text{ kNm} > M_{s-s} = 259.4 \text{ kNm}, \text{ OK. At service, } M_{s-y}/(f_c'bd^2) = 0.217$$

At ultimate load, the top concrete crushes. Using an ultimate compressive strain of 0.003, section analysis yields:

$$x = 152.0 \text{ mm}; F_{cc} = 1104.4 \text{ kN}; F_{sc} = 101.1 \text{ kN}; F_{st} = 580.4 \text{ kN}; F_p = 625.2 \text{ kN}.$$

$$M_{s-u} = 392.9 \text{ kNm} > 389.1 \text{ kNm}, \text{ OK; At ultimate state, } M_{s-u}/(f_c'bd^2) = 0.266$$

REFERENCE

- [1] Ross, C.A., Jersome, D.M., Tedesco, J.W. and Hughes, M.L. (1999). "Strengthening of reinforced concrete beams with externally bonded composite laminates", *ACI structural Journal*, 96(2), 212-220.

- [2] Rahimi, H. and Hutchinson, A. (2001). "Concrete Beams with Externally Bonded FRP Plates", *Journal of Composites for Construction*, 5(1), 44-56.
- [3] Arduini, M., Di-Tommaso, A. and Nanni, A. (1997). "Brittle failure in FRP plate and sheet bonded beams", *ACI Structural Journal*, 94(4), 363-370.
- [4] Teng, J.G., Chen, J.F., Smith, S.T. and Lam, L. (2002). *FRP strengthened RC structures*. John Wiley & Sons, West Sussex, England.
- [5] Hout, N.A. and Lees, J.M. (2009) "Modelling of an Unbonded CFRP Strap Shear Retrofitting System for RC Beams" *Journal of Composites for Construction*, ASCE, 13 (4), 292-301.
- [6] Hsu, C.T.T., Punurai, W., Bian, H. and Jia, Y. (2003). "Flexural Strengthening of Reinforced Concrete Beams Using Carbon Fibre Reinforced Polymer Strips", *Magazine of Concrete Research*, 55(3), 279-288.
- [7] Jones, R., Swamy, R.N., and Charif, A. (1988). "Plate separation and anchorage of reinforced concrete beams strengthened by epoxy-bonded steel plates", *The Structural Engineer*, 66(5), 85-94.
- [8] Carpinteri, A., Cornetti, P. and Pugno, N. (2009). "Edge debonding in FRP strengthened beams: stress versus energy failure criteria", *Engineering Structures*, 31, 2436-2447.
- [9] Achintha, M. and Burgoyne, C.J. (2008). "Fracture mechanics of plate debonding", *Journal of Composite for Construction*, 12(4):396-404.
- [10] Guan, G.X. and Burgoyne, C.J. (2012). "Comparison of FRP plate debonding analysis using global energy balance approach with different moment-curvature models", Submitted to *ACI Structural Journal*.
- [11] Gunes, O., Buyukozturk, O. and Karaca, E. (2009). "A fracture-based model for FRP debonding in strengthened beams", *Engineering Fracture Mechanics*, 76:1897-1909.
- [12] Shah, S.P. and Carpinteri, A. (edit) (1991). *Fracture mechanics test methods for concrete – RILEM Reports 5*, Chapman & Hall.
- [14] Guan, G.X., Burgoyne, C.J. and Achintha, M. (2012). "Fracture analysis for FRP plate debonding based on global energy balance: parametric study", to be submitted to *Journal of Composite for Construction*, ASCE.
- [13] Bazant, Z.P. and Becq-Giraudon, E. (2002). "Statistical prediction of fracture parameters of concrete and implications for choice of testing standard", *Cement and Concrete Research*, 32, 529-556.
- [15] Buyukozturk, O., Gunes, O. and Karaca, E. (2004). "Progress on understanding debonding problems in reinforced concrete and steel members strengthened with FRP composites", *Construction and Building Materials*, 18(1):9-19.
- [16] Hognestad, E., Hanson, N.W. and McHenry, D. (1955). "Concrete stress distribution in ultimate strength design", *ACI Journal Proceedings*, 52(4): 455-480.